University of Nevada

Reno

Earthquake Swarm near Denio, Nevada, February to April, 1973

A thesis submitted in partial fulfillment of the requirements

for the degree of Master of Science in Geophysics

by

William D. Richins

August 1974

The thesis of William D. Richins is approved:

Thesis advisor

Department chairman

Dean, Graduate School

University of Nevada

Reno

August 1974

ACKNOWLEDGMENT

I would like to express my appreciation to Dr. Alan Ryall, thesis advisor and director of the University of Nevada Seismological Laboratory, for his help and encouragement. I would also like to thank Bruce Douglas and Indra Gupta, thesis committee members and William Savage, Keith Priestley, and Schuyler Schaff for their advice. The help of the entire staff of the Seismological Laboratory has been appreciated, particularly Walter Nicks for his technical advice.

This research was supported in part by the Advanced Research Projects Agency and monitored by the Air Force Office of Scientific Research, under contract F44620-72-0069; and in part by a Sierra Pacific Power Company grant-in-aid, number 183-23-00.

ABSTRACT

An investigation of historic earthquake activity in northwest Nevada shows that earthquake swarms are typical. Evidence suggests that these swarms are associated with geothermal activity. An earthquake swarm occurred during February, March and April, 1973, 20 kilometers south of Denio on the Nevada/Oregon border. The largest event of the sequence was a magnitude 5.3 shock on 3 March. Fault plane solutions indicate right-lateral oblique-slip motion on a plane striking N11°W and dipping 60°E. This mechanism is very similar to those of the 1954 Fairview Peak and other earthquakes in the western Basin and Range, and is consistent with regional extension in a WNW-ESE direction. During March and April, a small tripartite array recorded more than 1,500 events of this sequence, and 221 of these were selected for detailed analysis. Epicenters of these events fall in a north-south trending zone, 8 kilometers in length and 2 kilometers wide; focal depths range from 5 1/2 to 8 1/2 kilometers. The b-value for this sequence is 1.00 which is considerably higher than 0.81 found for northwest Nevada as a whole. High b-values have been found in laboratory experiments for heterogeneous materials and for rocks under low to moderate stress.

TABLE OF CONTENTS

LIST OF TABLES

LIST OF ILLUSTRATIONS

Page

INTRODUCTION

The main purpose of this investigation was to analyze in detail an earthquake swarm which occurred in northwest Nevada south of Denio on the Oregon border beginning in late February, 1973. This type of activity is typical of northwest Nevada, and it was hoped that such an investigation would give some insight into the seismicity of that part of the state. Due to the remoteness of the earthquake swarm, only approximate locations can be expected using the statewide permanent seismic network operated by the University of Nevada. In order to obtain precise locations of the small events of the swarm, a six-component tripartite array was set up in the field and operated for approximately six weeks. Earthquake distribution, rate of occurrence, and mechanism of faulting will be discussed.

Recently, northwest Nevada has become an area of economic interest, both in terms of possible sites for nuclear reactors and possible geothermal resources. The historic seismicity and the possible connection of earthquake swarms with geothermal activity will be discussed for this part of Nevada. The results will then be compared with earthquakes in central and southern Nevada.

Chapter 1

SEISMICITY OF NORTHWEST NEVADA AND THE POSSIBLE RELATIONSHIP BETWEEN EARTHQUAKE SWARMS AND GEOTHERMAL ACTIVITY

Historic Earthquake Activity in Northwest Nevada. Historically, earthquake activity in northwest Nevada has been characterized by swarms of earthquakes, each concentrated in an area of a few square kilometers and lasting several months. Typically, these swarms consist of a buildup of activity, both in number and magnitude of individual events, over a period of a few days or weeks, climaxed by many events of nearly the same size without a distinct main shock. The large events generally have magnitudes around 5.0. Activity then dies off at a much slower rate than the rate of buildup, lasting several months on the average.

This type of activity differs considerably from that of western Nevada. In that part of the state, great earthquakes ($M > 7$) occur, followed by up to 100 years of aftershock activity; as illustrated by the 1915 Pleasant Valley, the 1932 Cedar Mountains, and the 1954 Fairview Peak - Dixie Valley earthquakes. Generally, earthquakes with magnitude less than 5.0 occur either in these aftershock zones or as isolated events with little or no foreshock or aftershock activity. Swarms also occur in the western Basin and Range, especially in the Fish Lake Valley region. Beginning in late October, 1964, an earthquake swarm occurred in Fish Lake Valley, the largest event having a magnitude of 4.7. Over 30 events were felt in the small town of Dyer. This area had another small swarm in March, 1971, with the largest events having magnitudes of 3.0 to 3.8. Central Nevada also had a

swarm sequence near Rawhide in October, 1971. Earthquake swarms in western Nevada, however, appear to be only a minor part of the earthquake activity, with main shock-aftershock sequences and isolated events much more common.

Figure 1 shows earthquakes in Nevada for the three-year period from 1970 to 1972, located by the University of Nevada Seismological Laboratory. The zone of high activity in west-central Nevada represents aftershock activity associated with the 1954 Fairview Peak - Dixie Valley earthquakes. The areas near the 1915 Pleasant Valley, the 1932 Cedar Mountains and the 1934 Excelsior Mountains earthquakes also represent active regions of the state. The location of these earthquakes can be seen in figure 1. Note the general lack of activity in northwest Nevada as compared to central and southern Nevada.

Recently, historic earthquake activity in northwest Nevada has been studied in detail by Dr. Alan Ryall of the University of Nevada Seismological Laboratory, as part of a nuclear reactor siting study supported by a grant-in-aid from Sierra Pacific Power Company (Ryall and Douglas, 1974). The first seismograph station in Nevada was installed in Reno at the Mackay School of Mines in 1916. Information on earthquakes for the pre-instrumental period, 1840 to 1916, was obtained from published earthquake catalogs, and from accounts published in various newspapers throughout northern Nevada. According to Ryall, it is doubtful that any earthquakes with magnitude greater than about 5.5 in northwest Nevada have been missed for the period after about 1860. Instrumental recordings of earthquakes for the period 1917 to 1969 are

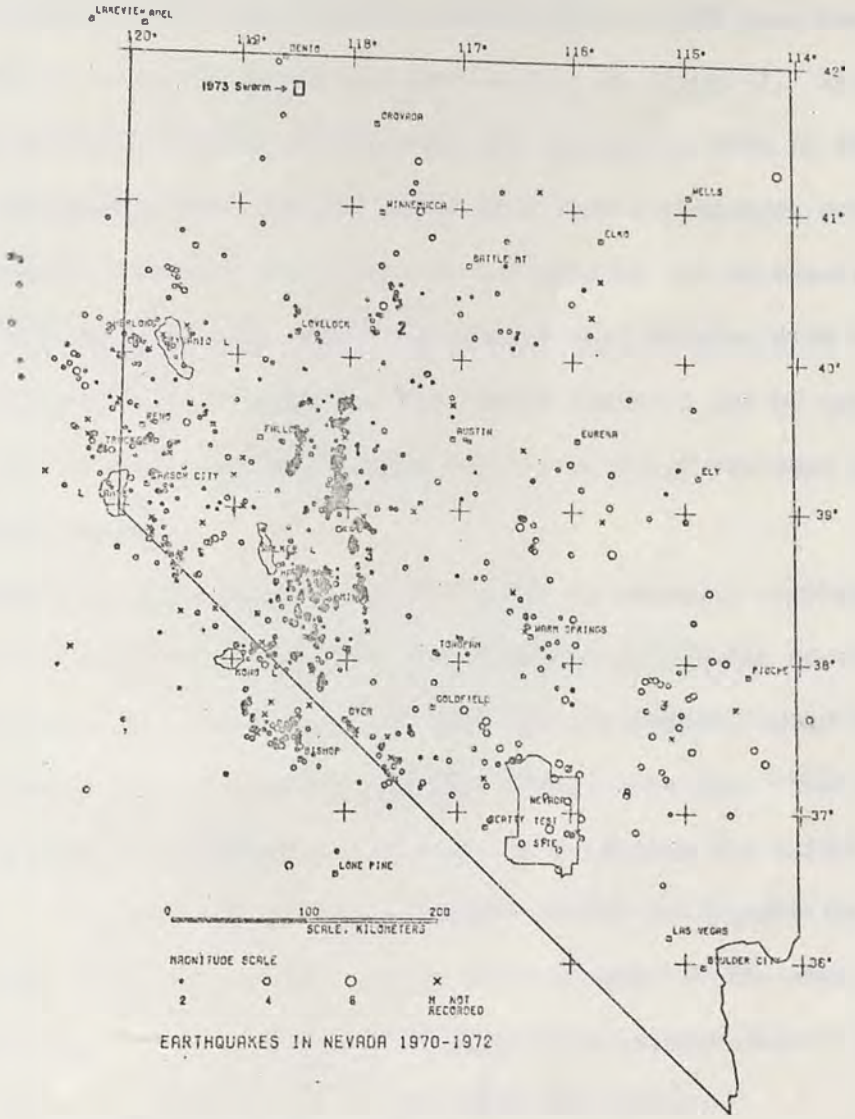

Figure 1. Earthquakes in the Nevada region for 1970-1972. Data from the University of Nevada seismic network. Location of the 1973 Denio swarm epicenter map is shown. 1 -- 1954 Fairview Peak-Dixie Valley earthquakes, 2 -- 1915 Pleasant Valley earthquake, 3 -- 1932 Cedar Mountains earthquake, 4 -- 1934 Excelsior Mountains earthquake.

available from various sources and the locations and magnitudes have been recalculated for many of these events.

Earthquakes for the historic period 1860 to 1969 have been plotted on a map of northwest Nevada and can be seen in figure 2. Ryall also plotted northwest Nevada earthquakes for the period 1970 to 1972. These earthquakes were located using data from a statewide network of seismographic stations installed and operated by the University of Nevada beginning in late 1969. Epicenters were located with an accuracy of about $\pm$ 10 kilometers. The events analyzed can be seen in figure 3. Most of the larger open circles on these two maps represent earthquake swarms.

From this data, Ryall concluded that, in general, earthquake activity in this part of the state has remained relatively constant for the past century. Areas that now have microearthquake activity had larger earthquakes during the 110 year historic period. Several areas that are presently aseismic have remained so during the entire historic period. If we exclude the 1915 Pleasant Valley earthquake (magnitude about 7.8) which was located at the southern edge of the area under consideration, no earthquakes with magnitudes greater than 5 3/4 have occurred in northwest Nevada during historic time.

Recurrence curves (refer to section on recurrence curves, b-values, and magnitudes in chapter 2) have been plotted by Ryall and Douglas (1974) in figure 4. Curve A is for an area of 140,000 square kilometers in northwest Nevada for the period 1970 to 1972 and has a slope or b-value of 0.81. Curve B is for a region of approximately the same area (143,000 square kilometers) in central Nevada for the same period and

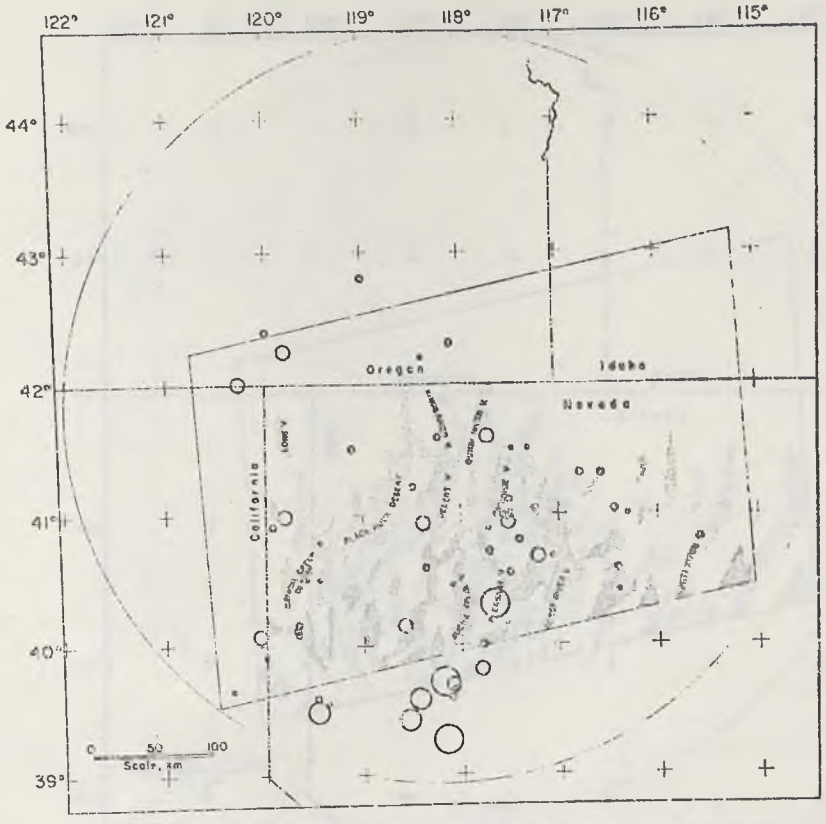

Figure 2. Earthquakes in northwest Nevada from about 1860 to 1969. (From Ryall and Douglas, 1974).

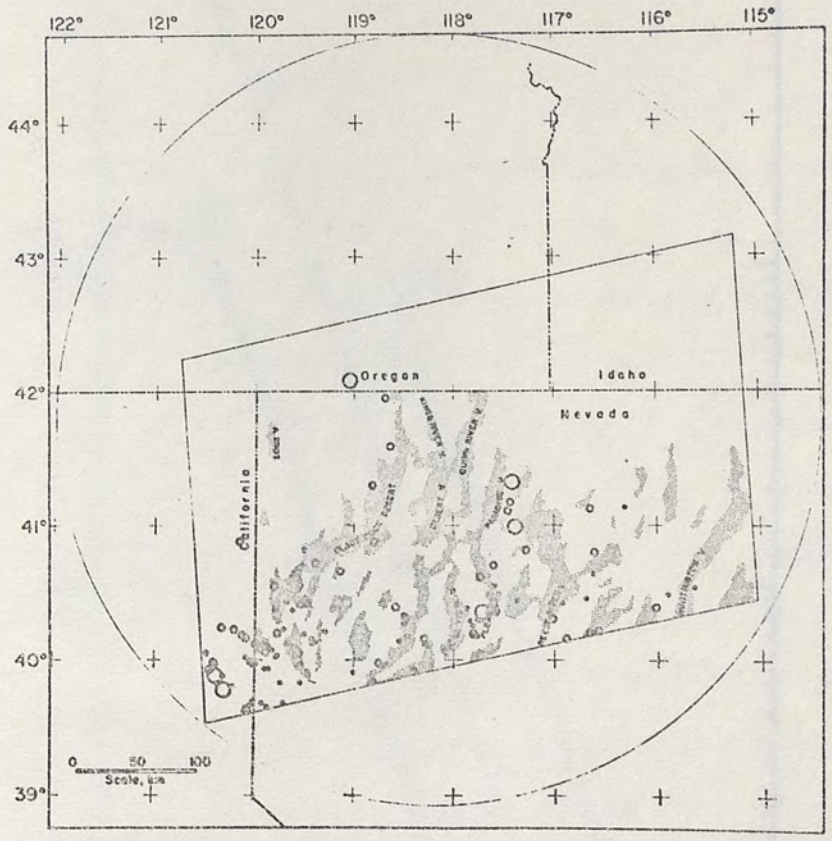

Figure 3. Earthquakes in northwest Nevada from 1970 to 1972. (From Ryall and Douglas, 1974).

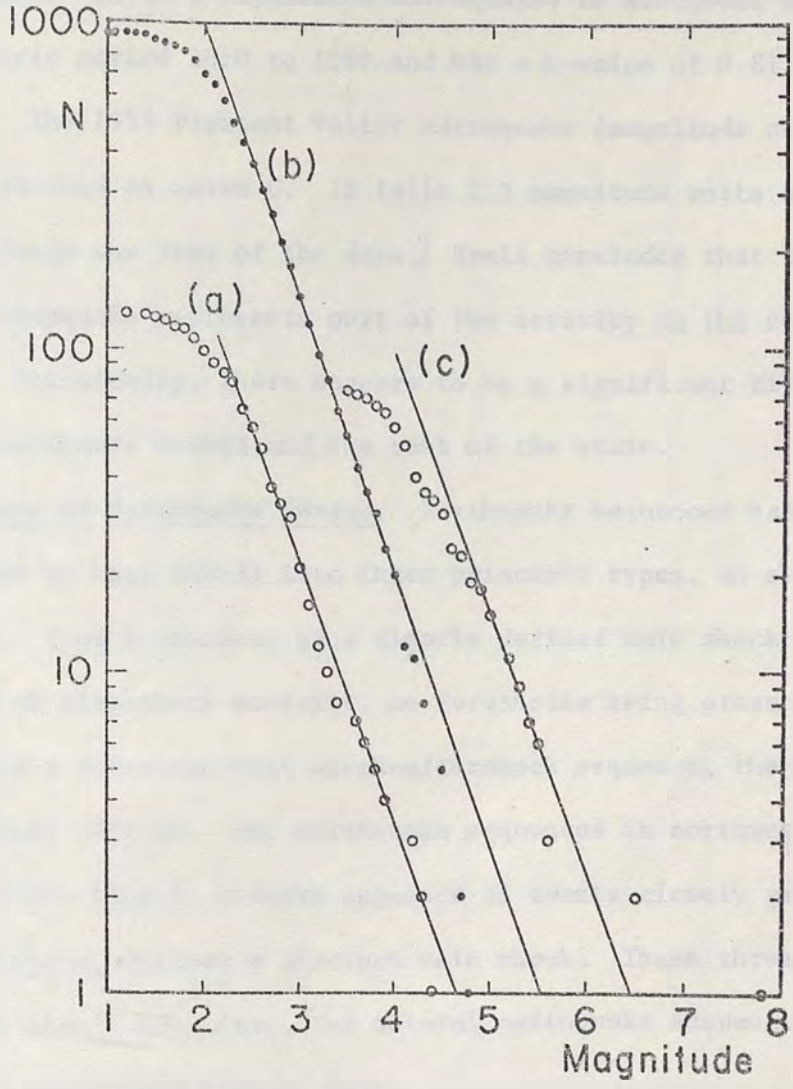

Figure 4. Recurrence curves. N is the number of earthquakes with magnitude $\geq$ M. (A). Northwest Nevada, 1970 to 1972; (B). Western Nevada, 1970 to 1972; (C). Northwest Nevada, 1860 to 1969. (From Ryall and Douglas, 1974).

has a b-value of 0.85. Note that the rate of seismic activity for northwest Nevada is down by more than a factor of 5 as compared to central Nevada. Curve C represents earthquakes in Northwest Nevada for the historic period 1860 to 1969 and has a b-value of 0.81, the same as curve A. The 1915 Pleasant Valley earthquake (magnitude about 7.8) can be seen plotted on curve C. It falls 1.3 magnitude units off the line drawn through the rest of the data. Ryall concludes that the Pleasant Valley earthquake represents part of the activity in the central Nevada region. Seismically, there appears to be a significant difference between northwest Nevada and the rest of the state.

Causes of Earthquake Swarms. Earthquake sequences have been classified by Mogi (1963) into three principle types, as shown in figure 5. Type 1 consists of a clearly defined main shock followed by a period of aftershock activity, no foreshocks being present. Type 2 represents a foreshock-main shock-aftershock sequence, the main shock also clearly defined. The earthquake sequences in northwest Nevada appear to fit type 3, a swarm sequence of events closely grouped in time and space, without a distinct main shock. These three classifications are highly idealized, and natural earthquake sequences are in general a graduation between them.

Laboratory studies of the microfracturing of rock show that inhomogeneities in the stress field caused either by concentrated sources or inhomogeneous materials, are correlated with swarm-like sequences similar to Mogi's type 3, having relatively high b-values (Mogi 1963, Scholz 1968a). According to Mogi (1963), type 3 sequences occur in highly fractured and otherwise heterogeneous regions. The applied

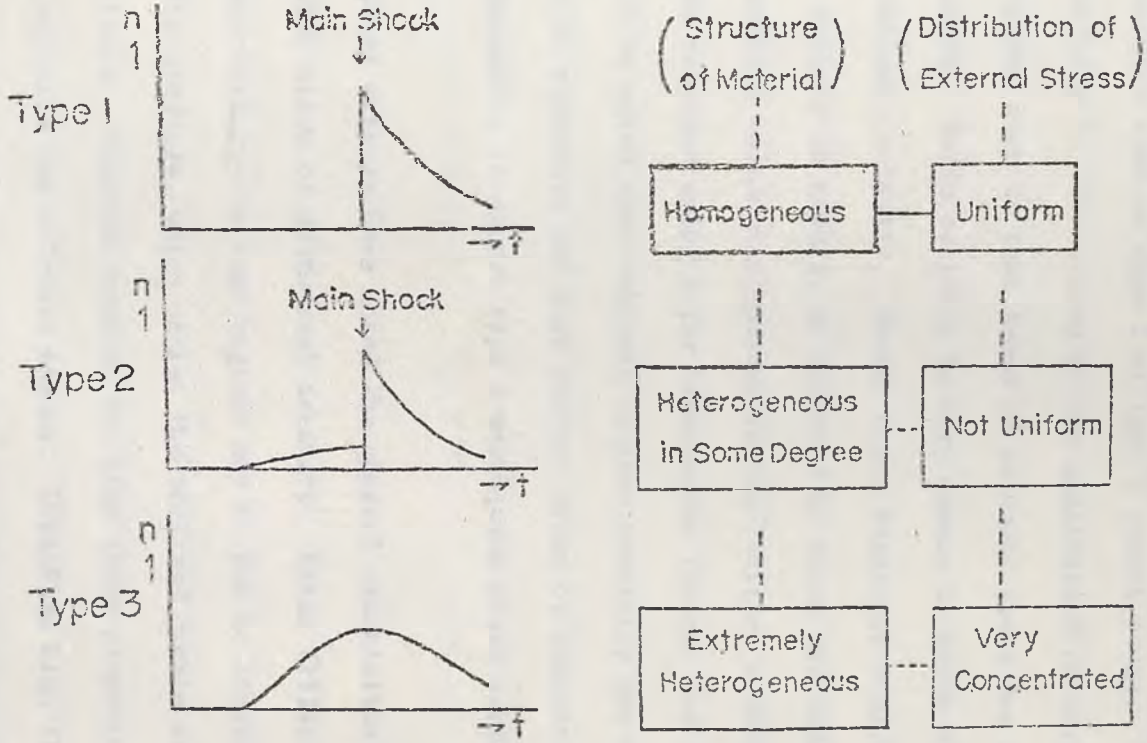

Figure 5. Three classifications of earthquake sequences as a function of time t. n is the number of events per unit time. Conditions producing these three types in the laboratory can be seen at the right. (From Mogi, 1963).

stress is relieved along numerous cracks and faults, and local fractures occur in areas of relatively low stress. The result is that regional stresses cause numerous small- to moderate-sized earthquakes, and a large buildup of stress which would lead to a main shock-aftershock sequence such as type 1 or type 2 cannot occur. This type of swarm activity is also caused by the application of extremely concentrated stress such as that found in volcanic areas due to the intrusion of hot magma. Swarm activity is very common in areas with current or recent volcanic activity. Swarms occur regularly near the summit of Kilauea Volcano in Hawaii, as reported by Eaton and Murata (1960). During several volcanic eruptions in the Pacific, earthquake swarms have been recorded using Sofar hydrophones (Norris and Johnson, 1969). It should be noted that volcanic regions generally are extremely heterogeneous in structure and also contain areas of concentrated stress. It is reasonable to expect type 3 earthquake swarm activity in these regions.

Several workers have noted the general association of earthquake swarms with areas of geothermal activity. Sykes (1970), postulated that swarm activity in some regions may be due to localized sources of high fluid pressure, which weaken the rock and create areas of concentrated stress. Possible sources for high fluid pressure include hydrothermal activity and volcanic magmas. Localized high fluid pressure was undoubtedly the cause of the man-made Denver earthquakes (Healy *et al.*, 1968). Ward and Bjornsson (1971), in their study of swarms and microearthquake activity in Iceland concluded that stress along a transform fault in southern Iceland is relieved by earthquake swarm

activity in the geothermal areas and by main shock-aftershock sequences elsewhere on the island. The microearthquakes they recorded were located in 13 zones each less than 10 kilometers in diameter. Nine of these zones of activity occur in regions of major geothermal action, while two other zones occur in regions of historic submarine volcanism that may have associated geothermal activity. Most of these events had focal depths between 2 and 6 kilometers.

It is possible that swarms also occur in regions where the crust is weakened to the point where only moderate sized stresses can be sustained. The stress would then be relieved by numerous small earthquakes. The effects of fluids, fluid pressure, and chemical alteration found near areas of geothermal activity could be a source for this weakening. Water in geothermal areas probably circulates to depths of several kilometers. Such water causes stress corrosion as described by Scholz (1968b), which creates far greater weakening at high temperature than at normal temperatures. These fluids, circulating along cracks and faults, also leach out material such as silica, weakening the rock still further. It is reasonable to assume that fluids do circulate to the depths of the earthquakes of the Denio swarm discussed here.

Figure 6 shows a map of heat flow measurements in the western United States taken from a paper by Sass et al., (1971). The cross-hatched area in north-central Nevada represents a region known as the Battle Mountain heat flow high. Heat flow values in this region are generally greater than 2.5 H.F.U., with values as high as 3.8 H.F.U. This part of Nevada is an area with perhaps the highest heat flow in the western United States. While heat flow measurements have not been

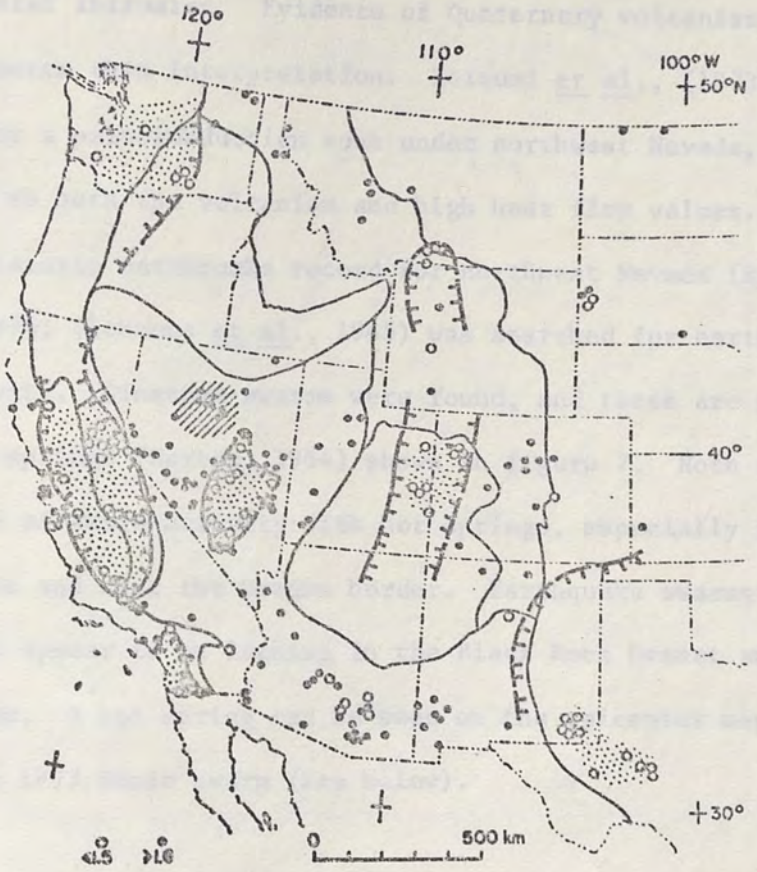

Figure 6. Heat flow measurements in the western United States. Stippled areas have heat flow of 1.5 or less; the heavy lines are 1.5 H.F.U. contours. The cross-hatched area has heat flow greater than 2.5. (From Sass et al., 1971).

made for the rest of northwestern Nevada, it seems likely that most of northwest Nevada is an area with high heat flow. Sass et al., (1971) interpret the Battle Mountain heat flow high as the effect of a fairly recent crustal intrusion. Evidence of Quaternary volcanism in the region supports this interpretation. Koizumi et al., (1973) found evidence for a paleosubduction zone under northwest Nevada, which might be related to both the volcanism and high heat flow values.

The historic earthquake record for northwest Nevada (Ryall and Douglas, 1974; Slemmons et al., 1965) was searched for earthquake swarm activity. Nineteen swarms were found, and these are plotted on a map of hot springs (Horton, 1964) shown in figure 7. Note the general association of swarm activity with hot springs, especially in the Gerlach area and near the Oregon border. Earthquake swarms as well as hot springs appear to be lacking in the Black Rock Desert and Desert Valley areas. A hot spring can be seen on the epicenter map in the area of the 1973 Denio swarm (see below).

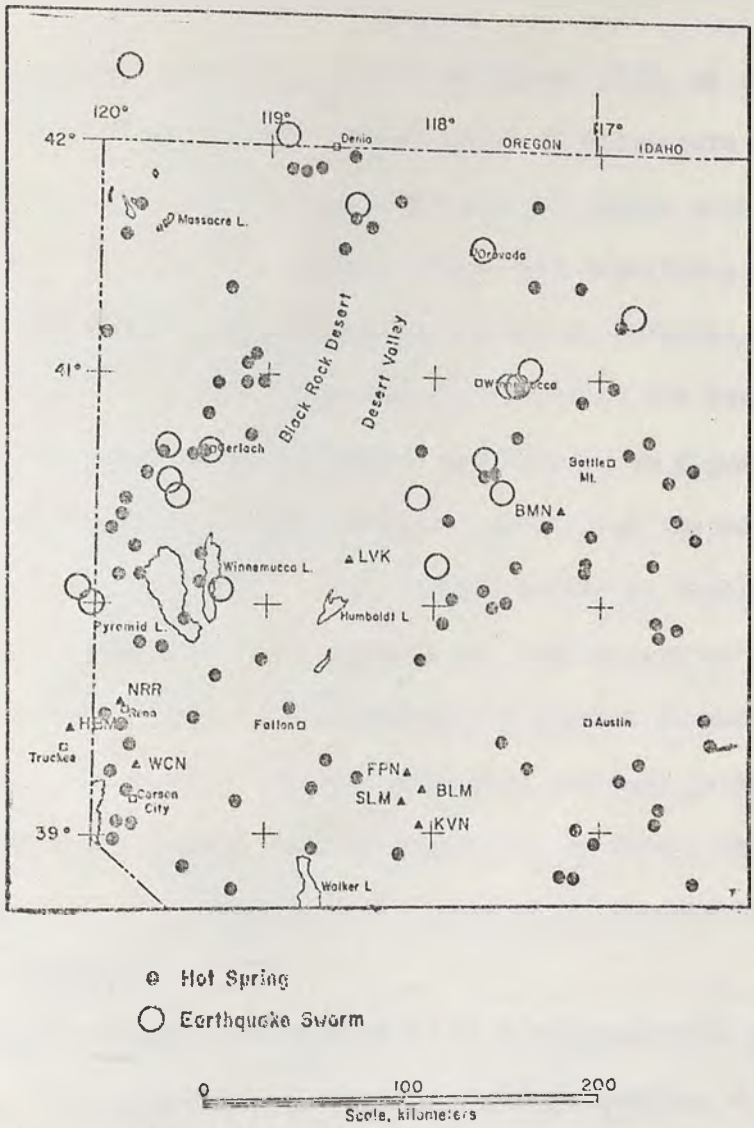

Figure 7. Earthquake swarms and hot springs in northwest Nevada.

Chapter 2

THE DENIO EARTHQUAKE SEQUENCE OF FEBRUARY TO APRIL, 1973

Introduction. Beginning in late February, 1973, an earthquake sequence occurred in northwest Nevada about 20 kilometers southeast of Denio, Nevada. This sequence included over 60 events with magnitude greater than 2 and the four largest events had magnitudes of 5.3, 5.1, 4.7, 4.7. The staff of the University of Nevada Seismological Laboratory conducted field investigations shortly after the large events. The general location of this sequence can be seen in figure 1.

The 1973 Denio earthquake swarm was located on the western slope of the Bilk Creek Mountains, which consist mainly of Tertiary basaltic and andesitic rocks with some rhyolite and dacite present (Langenheim and Larson, 1973). This type of geology is typical of much of northwest Nevada. The area is one of complicated volcanic geology, extremely high heat flow, a great deal of geothermal activity, and appears to be characterized by earthquake swarm activity as opposed to main shock-aftershock sequences.

Some minor damage was reported to be associated with the largest events. At the Quinn River Highway Maintenance Station, 8 kilometers southwest of the center of activity shown on figure 1, the following damage was observed: concrete-block pump shed, approximately 12' x 20' with concrete slab roof, had cracks on all four corners; a fuel tank, 6' - 7' long, on a braced angle-iron mounting approximately 5' high, moved one inch toward the east; a second tank, about 12' long on a 7' high concrete block stand, moved 1/4" toward the east; concrete slab floors in the basement of a one-year-old house were cracked, although a

slab floor in the older maintenance station garage did not crack; a ceiling was slightly separated from the walls; and dishes fell from cabinets. At Bramlett Well, 5 kilometers southwest of the center of activity, two large cattle watering tanks were shifted back and forth in the ground in a WNW-ESE direction, leaving a gap of about 1" in the dirt on the two sides of the tanks; a power pole had also moved back and forth, leaving a gap of about 1/2" in the dirt on both sides of the pole. The large event was felt in Winnemucca, 120 kilometers to the southeast.

The center of activity was originally located using a portable recording system consisting of an Electrotech EV-17 seismometer and a Geotech Helicorder. Distances from several recording sites to the earthquakes were approximated using S-P times. From this information, a site for the installation of a small tripartite array was chosen.

The geometry of the array can be seen in figure 8. Each station consists of a vertical short-period seismometer connected by wire to the recording system at the SYC site. In addition to the vertical instruments, two horizontal short-period seismometers oriented north-south and east-west were placed at the SYC station. The geographic coordinates of the center of the array are: 41.7869°N, 118.5090 W.°

Instrumentation. The portable field seismic unit used to obtain data for this investigation is mounted in a heavy plywood box and was buried just below ground level. The box is divided into two compartments; one compartment houses a seven-channel, slow-speed tape recorder (Geotechnical Corporation model 17373), and the other contains six Geotech model AS-330 solid-state seismic signal amplifiers. The box

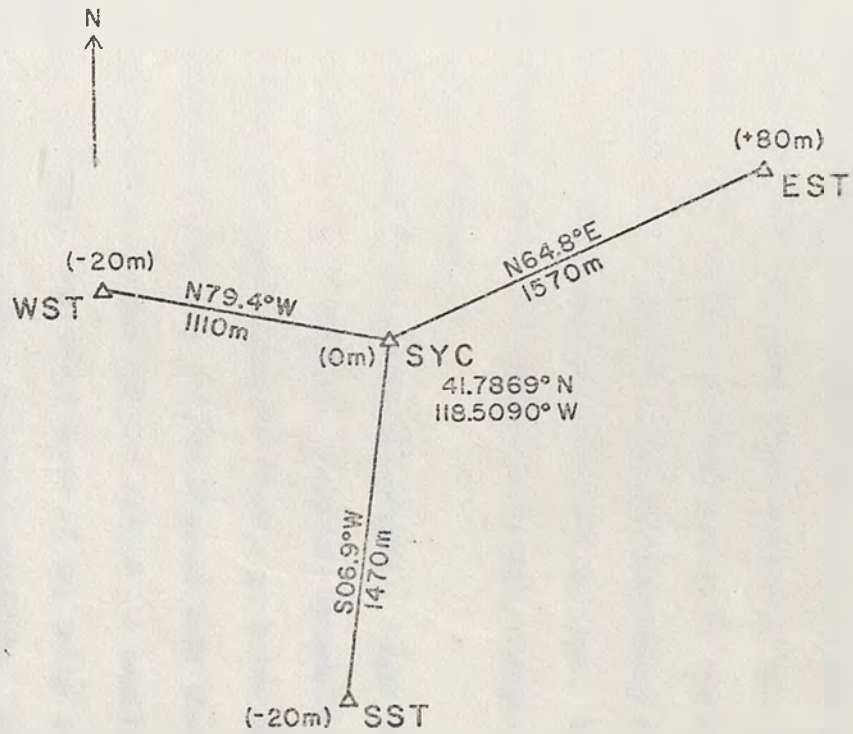

Figure 8. Geometry of the tripartite array used to monitor the 1973 Denio earthquake sequence.

also holds a Develco model 3202A radio time code receiver, which receives continuously the time code broadcast from Radio Station WWVB in Fort Collins, Colorado. Located just outside the box are ten 2 1/2-volt air-cell batteries used as a power source.

Three vertical seismometers (Mark Products, Inc. model L-4), and a three component set consisting of one vertical and two horizontals placed north-south and east-west (Mark Products, Inc. model L-4-30) are connected by wire to the recording system in the box. A monitor panel is provided in the box to allow for monitoring of the seismic signals before and after they are recorded on tape. The system will record for approximately ten days between tape changes, and three months on a set of batteries.

The system used to play back the magnetic tapes recorded in the field is located at the University of Nevada Seismological Laboratory in Reno. A Bell and Howell type VR-3700B tape drive with VR-2800 playback electronics was used and the signals were then fed into a Siemens Oscillomink U sixteen-channel liquid jet oscillograph.

Analysis of Data. The field tapes of the Denio earthquake sequence were played back using a two-step procedure. First, each tape was played out continuously at 40 times recording speed, through the Siemens chart recorder. These records were then searched for good quality events to be used for detailed analysis. The continuous records were also used for counting the number of identifiable earthquakes per hour. Earthquakes picked for further study were then played out at 10 times recording speed, producing seismograms consisting of all six seismic signals and the WWVB time code. The chart-recorder paper speed

was chosen such that one second of real time measured approximately six centimeters.

A total of 221 events were picked for detailed analysis. P-wave arrival times could be read at all stations for most events, to the nearest 0.01 second. Nearly all events had surprisingly sharp S-phases. These arrivals were picked using the two horizontal seismometers at the SYC site, and could usually be read to the nearest 0.02 second. Several events were tested using the LOC computer program (see below), to see how these reading errors affect the hypocenter locations. By varying the P-wave arrival times and the S-P times within the expected reading error limits, the hypocenter varies by no more than 200 meters.

Since no detailed studies of velocity structure are available for this part of Nevada, certain reasonable assumptions must be made. Meister (1966), in his seismic refraction study of Dixie Valley in central Nevada, found a near-surface hard rock velocity of 4.7 km/sec for P-waves, to a depth of 2 kilometers. In a crustal refraction study between Fallon and Eureka, Eaton (1963) found a Pg velocity of 6.0 km/sec to a depth of about 31 kilometers. Stauder and Ryall (1967), in a paper on microearthquakes in the Fairview Peak area of central Nevada, used a two layer earth model consisting of a 4.7 km/sec layer 2 kilometers thick, over a 6.0 km/sec half space. This same velocity structure was applied here. A Poisson's ratio of 0.25 was assumed, giving S-wave velocities in the two layers of 2.7 and 3.5 km/sec.

After all earthquakes were played out, the Siemens chart recorder was checked to see that the ink jets were properly aligned. It was

discovered that the jet used for the SYC vertical trace caused an error of 0.03 seconds. When a station correction of this amount was applied to the SYC station, the P-wave arrival time residuals for most events were less than 0.005 seconds at all stations. It was therefore assumed that further station corrections were unnecessary, and the hypocenters were located as accurately as possible. This seems reasonable, as the four stations differ by no more than 100 meters in elevation, and the three westernmost sites can be expected to be on a greater amount of alluvium than the EST site.

The Location Routine. The computer program used to locate the micro-earthquakes recorded by the tripartite array is an adaptation of the HYPOLAYR program written by J. P. Eaton (1969) of the United States Geological Survey. This program, LOC, calculates the origin time using the S-P times at one or several stations, and using the station with the smallest S-P time, makes a first estimate of the hypocenter. Arrival times at each station are then computed from this trial hypocenter through an earth model of horizontal layers of constant P-wave velocity. The partial derivatives of the traveltimes with respect to the hypocenter coordinates are also computed. The trial hypocenter is then adjusted by Geiger's least-square method to minimize the residuals of observed arrival times versus computed arrival times. This process is continued until an iteration limit is reached, or until the hypocenter is adequately determined.

The program allows for station corrections (seconds) to be applied to the observed arrival time data. The user may fix the depth of each hypocenter at a given value, or allow the program to compute the depth along with the horizontal coordinates. The Geiger least-squares method

is discussed in detail in Appendix I, and a description of the CAL subroutine used to calculate the traveltimes and partial derivatives can be found in Appendix II.

Earthquake Distribution. The epicenters calculated using the LOC computer program are shown in figure 9. The zone of activity falls in a rectangular area, trending approximately north-south, 8 kilometers in length and 2 kilometers wide. The location of the field array can be seen as small open triangles on this figure. A vertical profile from A to A' along the direction of the fault plane solution discussed later, and a cross section from B to B' are plotted in figure 10, showing the depths of these earthquakes. Note the general clustering of the hypocenters in the vertical cross section, along a plane dipping about 60 degrees to the east as the fault plane solution suggests. Most events are between 5 1/2 and 8 1/2 kilometers in depth. The shallowest natural earthquake sequence observed in the Nevada region to date was the 1966 Truckee aftershock sequence (Ryall et al., 1968) which had depths between 3 and 7 kilometers. The depths found for the 1973 Denio swarm agree with those found for the 1968 Adel, Oregon swarm and the 1966 Caliente, Nevada sequence, which had a depth range of 5 to 10 kilometers (Ryall and Savage, 1969).

It should be noted that these earthquake locations depend on the velocity structure used in the analysis. Since this area has not been subjected to detailed geophysical investigation, a velocity structure typical of similar areas in central Nevada was used here. Using a different velocity structure would have the effect of displacing the sequence as a whole. As a result, the absolute locations may be good to

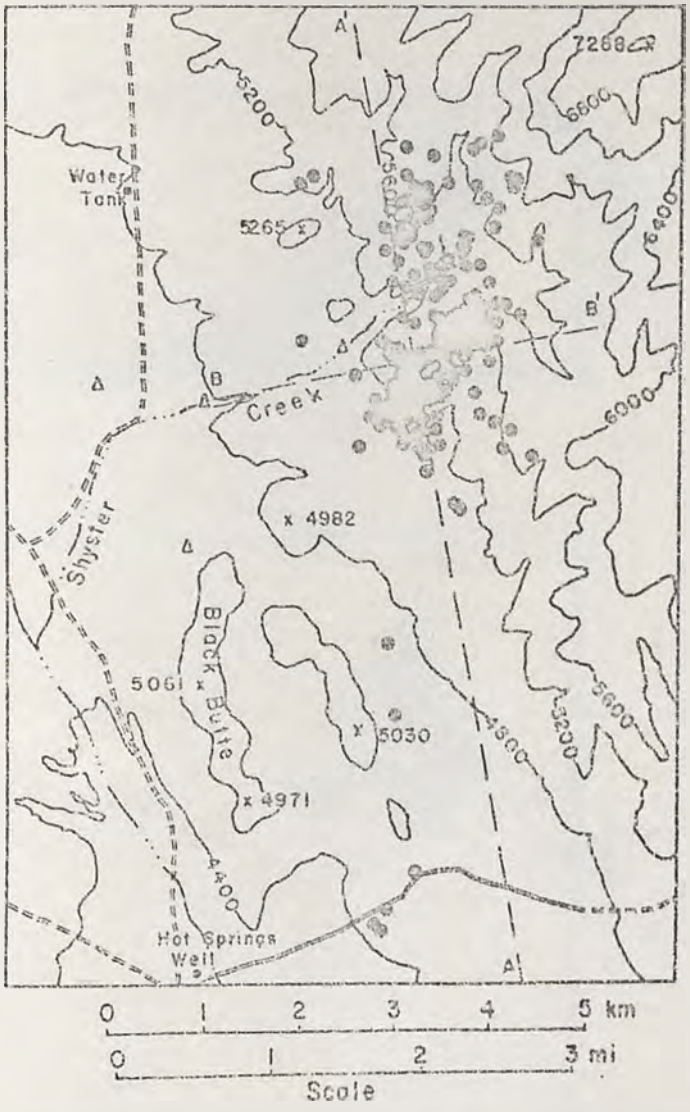

Figure 9. Epicenters of the 1973 Denio earthquake swarm. Small open triangles represent recording sites.

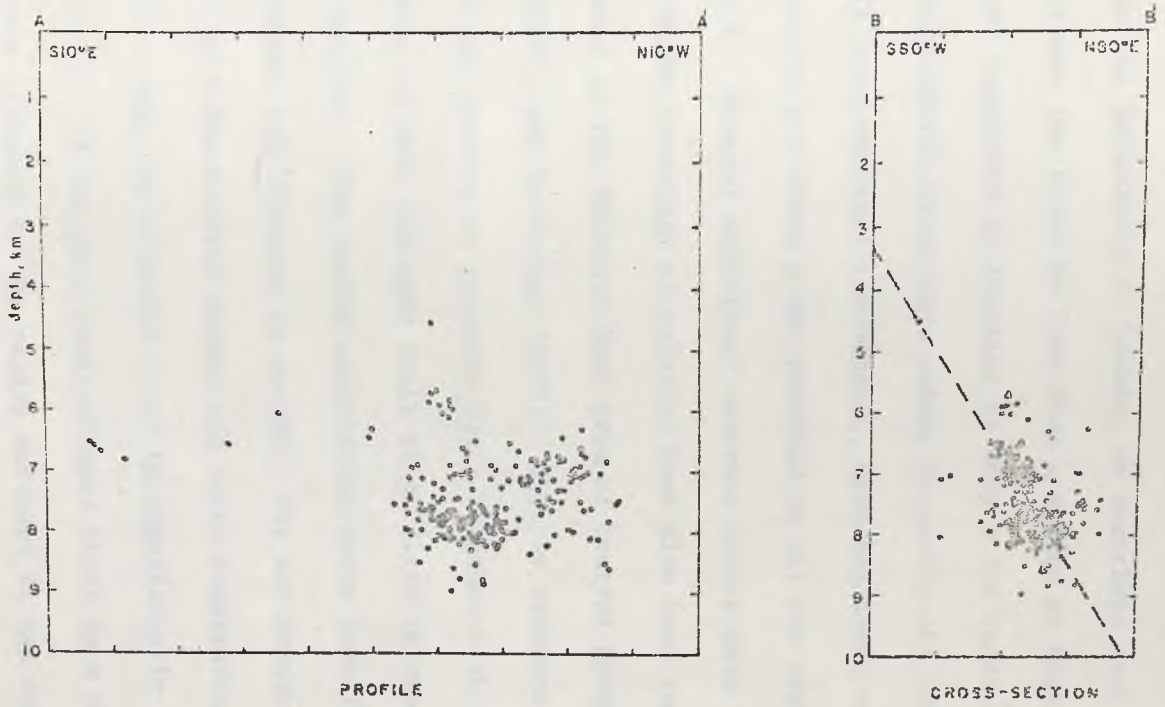

Figure 10. Depth profile and cross section of the 1973 Denio earthquake sequence. The fault plane solution is shown as a dotted line.

within about $\pm$ 1 kilometer, while the locations are subject to an error of less than 100 meters relative to each other.

Reversals of Polarity. Figure 11 shows two of the 221 located events recorded by the tripartite array and played out on the playback system at the University of Nevada, as described earlier. The second event follows the first by less than a minute in time, and the two events are separated in location by only a few hundred meters. Event A has first-motion directions common to nearly all events recorded -- up on all four vertical instruments, west and south on the horizontals. First motions for event B are reversed on all six traces when compared to event A. Several additional reversed events were found for this swarm. These reversals of polarity have also been seen for micro-earthquakes in the Fairview Peak area of central Nevada by Stauder and Ryall (1967), and by Savage (1972). This is evidence either that the two foci are located on separate fault branches with different slip directions, or that the main fault slips first in one direction and next in another. The second explanation seems doubtful when the two sample events are examined in detail. The two events are separated in location by a few hundred meters and their signatures differ somewhat. Also notice that the reversed event is significantly larger than the normal event. If the main fault slipped first in a direction dictated by tectonic stresses in the region and next in the opposite direction, the first event can be expected to have the largest motion. This is not the case here.

Rate of Occurrence. The temporal behavior of the 1973 Denio swarm was examined, using the continuously-recorded field data obtained from

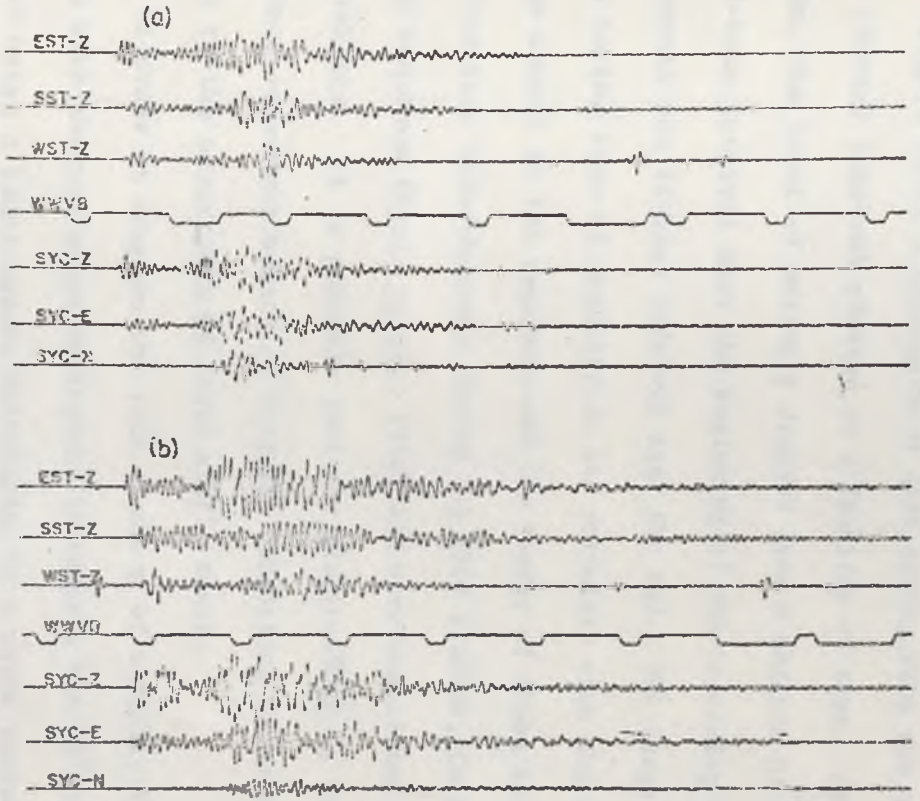

Figure 11. Sample events of the 1973 Denio earthquake sequence recorded by the tripartite array showing reversals of polarity. (a). March 16 06:28:03.11, (b). March 16 06:28:51.70.

the portable tripartite array. Unfortunately, recording began after the buildup and climax periods of the swarm, and only the dieoff period could be analyzed. Events on these records were counted for one-hour periods beginning March 7, 1973, three days after the climax period of the swarm and continuing through April 11, except for a few days during which no data is available due to tape recorder failure.

Figure 12 is a histogram of this swarm, with the number of events per 12-hour interval plotted as a function of time. As this figure shows, the level of activity dropped from a maximum of 217 events for a 12-hour interval near the beginning of the recording period, to about 10 events per 12-hour interval near the end. The large fluctuations seen in the rate of activity do not correlate with the occurrence of large events in the sequence and the source of these is unknown. Such fluctuations were observed during the 1966 Truckee, California earthquake sequence (Ryall et al., 1968) and were associated with large aftershocks. It is possible that the fluctuations in the 1973 Denio sequence represent bursts of activity consisting of many events as opposed to the occurrence of large single events.

In order to compare the rate of decay of activity for the Denio swarm with that of other earthquake sequences, the 12-hour counts were fitted using a least-square calculation to a curve representing hyperbolic decay. The equation resulting from this calculation is:

$$N(t) = 4140\ t^{-1.33}$$

Where N(t) = number of events per 12 hours and t = number of 12-hour periods after the largest event, 03:00:03 GMT on March 3, 1973

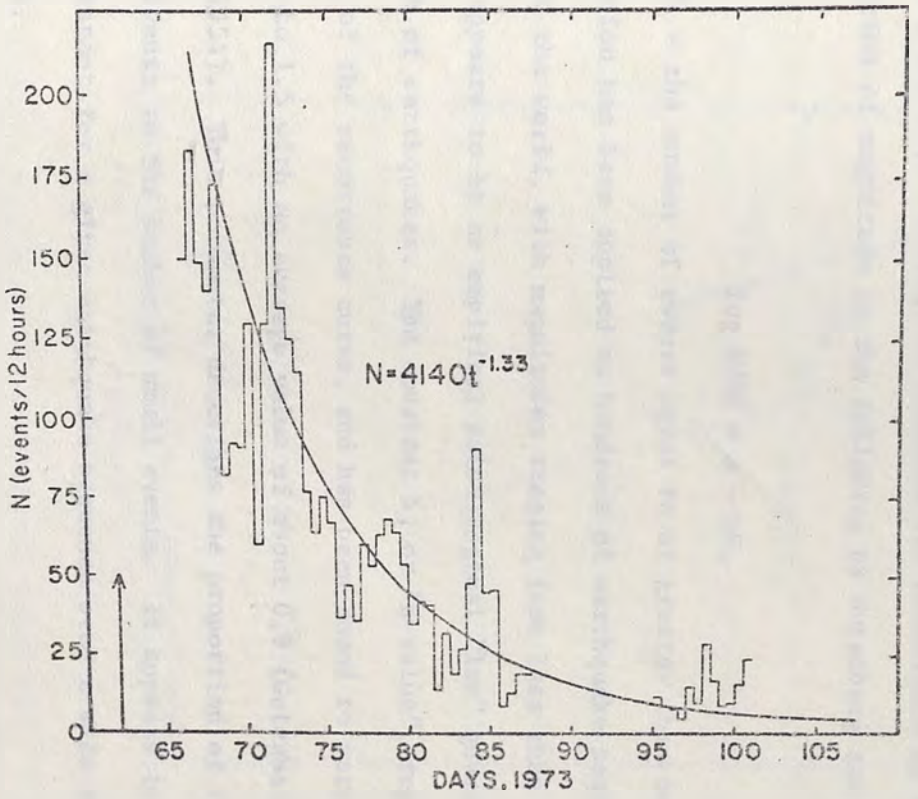

Figure 12. Histogram of the 1973 Denio earthquake sequence.

(M = 5.3). The value of the exponent, -1.33, indicates a considerably faster rate of decay than that normally found for aftershock sequences. A value of -0.64 was found for the 1966 Truckee aftershock sequence near Reno (Ryall et al., 1968). Values found for Japanese earthquake sequences range from -0.98 to -1.36 (Mogi 1962).

Recurrence Curves, B-Values, and Magnitudes. The formula most widely used for representing the frequency of occurrence of earthquakes as a function of magnitude is the following by Gutenberg and Richter (1944):

$$\log N(M) = a - bM,$$

where N(M) = the number of events equal to or greater than magnitude M. This equation has been applied to hundreds of earthquake sequences throughout the world, with magnitudes ranging from less than zero to 8.9, and appears to be an empirical seismological "law" governing the occurrence of earthquakes. The constant b, or "b value", represents the slope of the recurrence curve, and has been found to vary from about 0.5 to 1.5 with an average value of about 0.9 (Gutenberg and Richter, 1954). This parameter describes the proportion of the number of large events to the number of small events. It appears to be relatively constant for a given earthquake sequence over a wide range of magnitudes.

Microearthquake studies at various sites throughout the world usually show that the frequency of earthquakes increases approximately exponentially with decreasing magnitude, to a magnitude as low as -1 or -2 (Utsu 1971). Recurrence curves for the 1973 Denio earthquake swarm have been calculated and can be seen in figure 15. Curve A represents

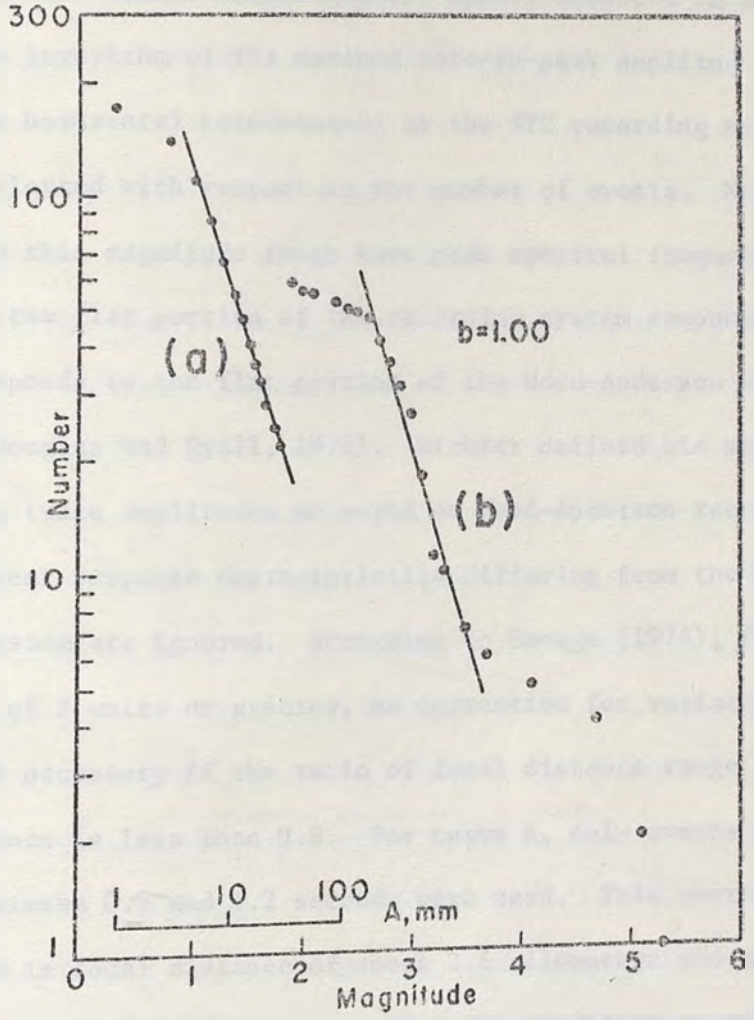

Figure 13. Recurrence curves for the 1973 Denio earthquake sequence. (a). Using amplitudes of events recorded by the tripartite array; (b). Using magnitudes from the permanent stations of the University of Nevada

data from the small tripartite field array using events with magnitude from approximately 0.5 to 2.0. A few days worth of recordings were taken as a sample. In order to avoid the difficulties encountered in calculating the Richter magnitudes for events recorded on the portable system, the logarithm of the maximum zero-to-peak amplitude, as measured on the horizontal seismometers at the SYC recording site for each event, is plotted with respect to the number of events. Microearthquakes with this magnitude range have peak spectral frequencies that lie within the flat portion of the recording system response, and this also corresponds to the flat portion of the Wood-Anderson seismometer response (Douglas and Ryall, 1972). Richter defined his magnitude scale using trace amplitudes measured on Wood-Anderson records. Thus the instrument response characteristics differing from the Wood-Anderson system are ignored. According to Savage (1974), for a magnitude range of 2 units or greater, no correction for variation in focal distance is necessary if the ratio of focal distance range to average focal distance is less than 0.8. For curve A, only events with S-P times of between 0.9 and 1.2 seconds were used. This corresponds to a variation in focal distance of about 2.5 kilometers and an average distance of about 9.0 kilometers. Thus the condition is satisfied.

Curve B represents magnitude data for larger events recorded by the permanent stations of the University of Nevada Seismological Laboratory, for the first month and a half of the swarm. These magnitudes were obtained by measuring the maximum trace amplitudes on horizontal components, and applying a conversion factor to convert these magnitudes to those found using the Wood-Anderson records from Reno.

Magnitudes thus computed are good to within about 0.2 of a magnitude unit. The peculiar shape of curve B from about magnitude 3.7 to 5.3 is probably due to the short time period of the sample. Smaller events, probably from this same area, have been detected for at least a year following the beginning of this swarm. Amplitude data for the rest of the swarm is not available, however. As the sequence is presently dying off, both in number and size of the events, large event activity is not expected; a longer time span would increase the number of small events, while the number of large events would remain the same. This would probably correct this part of the curve. The roll off near the top of both curves is due to the limit of detectability of each recording system. A list of the events used for curve B can be seen in table 1. It should be noted that only 60 events were available for use for curve B and that an accurate determination of b-value requires a greater data sample. Ryall et al., (1968), found that at least 100 events are needed to determine the b-value to 10 percent accuracy. The b-value derived from curve B is probably good to 20 or 25 percent accuracy. Both curve A and curve B give the same b-value when straight lines are visually fitted to the data and the accuracy should be about $\pm$ 0.10.

The largest events recorded by the tripartite array without clipping on the horizontals were several events of magnitude 1.9. The amplitude scale was thus lined up on this figure with the magnitude scale. Magnitudes recorded with the portable array ranged from approximately 0.3 to 1.9.

The b-value for both plots is 1.00, which is considerably higher than 0.81, the value for northwest Nevada as a whole (Ryall and Douglas,

1974). This is also higher than 0.81 for the Truckee aftershock sequence of 1966 near Reno (Ryall et al., 1968), 0.79 for the 1968 Adel, Oregon swarm (Ryall and Savage, 1969), 0.83 for the Caliente, Nevada aftershock sequence (Ryall and Savage, 1969), and 0.79 for the Ventura-Winnemucca seismic zone as a whole (Ryall et al., 1966).

Relatively high b-values have been found to accompany swarmlike sequences of microfracturing in rock (Mogi 1963, Scholz 1968a). Mogi (1966) showed that b increases with the degree of heterogeneity of the rock both in composition and in the density of the cracks. He measured the b-values for a sample of pine resin under triaxial compression. Pumice particles were placed in samples of pine resin in increasing quantities. It was found that increasing the ratio of pumice particles to pine resin medium (that is, increasing the degree of heterogeneity), increased the b-value. Mogi explained this by stating that the development of each fracture was interrupted by irregularities in the medium, either compositional or structural, and these limit the length of each fracture. This produces a larger ratio of small events to large events and increases the b-value.

Scholz (1968a) proposed a different interpretation to the physical meaning of high b-values in microfracturing experiments. He found that b depends strongly on the state of stress in the specimen and only to a lesser extent on its physical properties. He showed that b is inversely proportional to the effective stress and that high b-values are observed at low to moderate stress. This behavior was found at all pressures and for all types of brittle rock tested.

Wyss (1973) concluded that b is directly proportional to the local

TABLE 1

1973 DENIO EARTHQUAKE SWARM
LARGE EVENTS, LOCATION: 41.81 N, 118.48 W

Date	Origin Time	Magnitude
Feb. 25	11:33:57	2.9
Feb. 25	13:55:49	2.7
Feb. 25	14:19:45	3.2
Feb. 26	11:54:34	2.6
Feb. 26	13:11:36	2.6
Feb. 26	16:42:34	2.7
Feb. 26	20:17:04	3.0
Feb. 27	01:52:22	3.4
Feb. 27	02:19:23	2.6
Feb. 27	04:18:21	3.8
Feb. 27	04:21:09	2.8
Feb. 27	09:52:00	3.2
Feb. 27	12:35:38	3.2
Mar. 1	18:56:06	2.4
Mar. 2	11:28:41	5.1
Mar. 2	11:33:39	3.0
Mar. 2	12:06:13	3.3
Mar. 2	12:17:20	3.1
Mar. 2	14:14:06	4.1
Mar. 2	14:36:11	2.9
Mar. 2	14:47:16	1.9
Mar. 2	21:21:17	2.9
Mar. 3	03:00:03	5.3

Date	Origin Time	Magnitude
Mar. 3	03:15:50	3.0
Mar. 3	03:34:51	4.7
Mar. 3	03:43:25	2.9
Mar. 3	03:45:12	3.5
Mar. 3	04:03:25	2.8
Mar. 3	04:24:52	2.8
Mar. 3	04:28:40	2.6
Mar. 3	08:07:24	3.3
Mar. 3	08:10:06	2.6
Mar. 3	10:04:31	3.2
Mar. 3	14:26:54	2.9
Mar. 3	17:30:45	2.6
Mar. 3	18:52:04	4.7
Mar. 3	20:07:52	2.8
Mar. 3	20:08:29	2.3
Mar. 3	22:22:45	2.9
Mar. 4	01:27:05	2.7
Mar. 6	10:49:50	3.0
Mar. 6	10:50:32	2.5
Mar. 7	11: 47:47	2.6
Mar. 8	22:40:31	2.3
Mar. 9	00:18:30	2.1
Mar. 9	03:30:57	3.0
Mar. 9	09:53:15	3.0
Mar. 11	10:34:39	2.1

Date	Origin Time	Magnitude
Mar. 12	00:01:49	2.5
Mar. 12	02:26:37	2.7
Mar. 14	18:30:10	2.8
Mar. 14	22:10:32	2.7
Mar. 15	14:00:39	1.9
Mar. 15	15:24:36	1.9
Mar. 16	04:05:17	2.0
Mar. 22	09:14:31	2.1
Mar. 24	23:51:12	2.7
Mar. 24	23:57:21	2.7
Mar. 25	11:54:01	2.9

pore pressure. The Denver earthquakes which were triggered by the injection of waste fluids showed a strong correlation between b-values and pressure in the well (Healy et al., 1968). During the years of high fluid pressure, the b-values averaged about 0.85. In the years of low fluid pressure, b dropped to about 0.62. Wyss showed that this fits his theoretical work as well as the observations of Scholz (1968a), that b is inversely proportional to the state of stress.

The 1973 Denio earthquake swarm had a b-value of 1.00, which is considerably higher than 0.81 for northwest Nevada as a whole. Assuming that this swarm is connected with geothermal activity, this high b-value can be explained by the high local pore pressure. The rock in this area is extremely heterogeneous, consisting mainly of volcanics, therefore Mogi's explanation would also seem to fit. Noting that this seems to be an area where swarm sequences occur, as opposed to large events, only low to moderate local stresses exist. Thus a higher b-value can be expected as described by Scholz (1968a).

Mechanics of Faulting. Due to the location of the tripartite array and the close spacing of the recording sites, it was not possible to obtain fault mechanism information from the field data. As a result, near-regional Pn and Pg first motions were picked for three of the largest events occurring on 3 March, from the records of permanent stations in Nevada and nearby states. A list of the stations used can be found in table 2. Lower hemisphere plots of these first motions were made on an equal-area projection and can be seen in figure 14.

The fault-plane solution indicated by these three events is one with right-lateral, oblique-slip motion on a plane striking N11°W and

TABLE 2

STATION	Code	STATE	AZIMUTH	Pn Motion		
				03:00	03:34	18:52
Bell Mt.	BLM	Nevada	173.1		D	
Battle Mt.	BMN	Nevada	144.3	C	C	D
Blue Mt.	BMO	Oregon	15.6	C	C	C
Cedar City	CCU	Utah	132.4	C		
Corvallis	COR	Oregon	310.0	C		
Dugway	DUG	Utah	108.6	C		C
Fickle Hill	FHC	Calif.	258.3	C	C	C
Friant	FRI	Calif.	191.4			C
Granite Mt.	GMU	Utah	101.3			C
	HPI	Idaho	62.5	C	C	
Jamestown	JAS	Calif.	201.8	D	D	
Kaiserville	KVN	Nevada	173.5	D	D	D
Big Lost River	LRI	Idaho	65.0	C	C	C
Lovelock	LVK	Nevada	180.7	D	D	D
Mineral	MIN	Calif.	239.3	D		
Mina	MNV	Nevada	175.4	D	D	D
North Reno	NRR	Nevada	205.2	D		D
Worthington Pk.	NRWP	Nevada	149.2	D	D	
Oroville	ORV	Calif.	226.5	D	C	D
Ricks College		Idaho	65.6	C	C	
Shuckson	SHU	Wash.	343.6	C		
Slate Mt.	STM	Nevada	175.0	D	D	D
Tonto Hills	THO	Arizona	144.4	D		
	TMI	Idaho	70.6	C	C	C
Tonopah	TNP	Nevada	164.7	D	D	D
Tucson	TUC	Arizona	144.5	D		D
Uinta Basin	UBO	Utah	99.4	C	C	C
Washoe City	WCN	Nevada	201.5	D	D	C

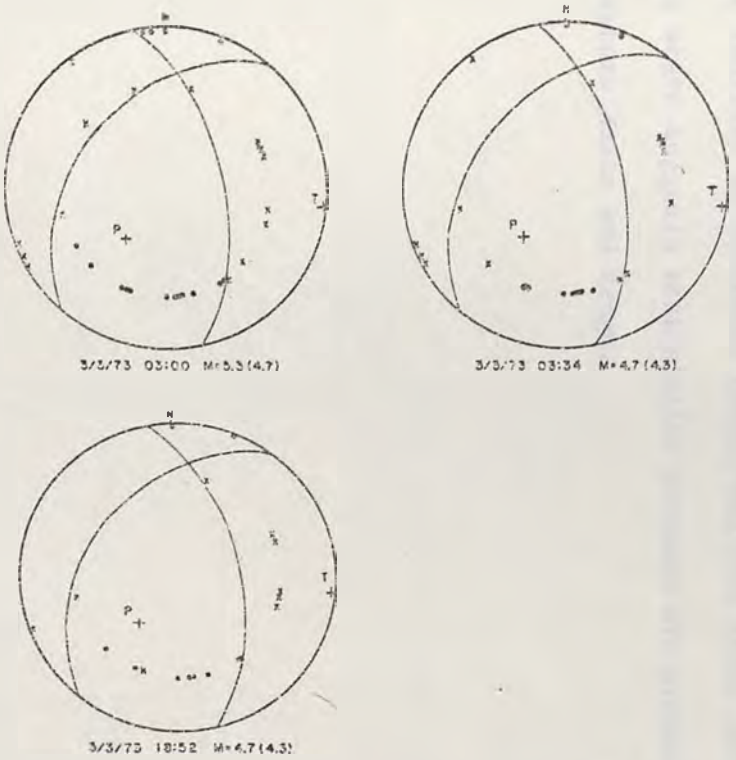

Figure 14. Fault plane solutions for three events of the 1973 Denio earthquake sequence. Magnitudes given are from Wood-Anderson records in Reno, Nevada. Magnitudes in parentheses are from the National Earthquake Information Center, Boulder, Colorado.

and dipping 60° to the east. The axis of maximum compression (P) trends S41°W with a plunge of 58°. The axis of minimum compression (T) trends S83°E with a plunge of 03°. This mechanism is very similar to those of the 1954 Fairview Peak and other earthquakes in the western Basin and Range Province, and is consistent with observed regional extension in a WNW-ESE direction. Figure 15 shows several earthquake mechanism plots for western Nevada. The similarity between the mechanism of faulting in northwest Nevada and that found throughout the rest of the state suggests that similar stresses are presently operating in the western Basin and Range.

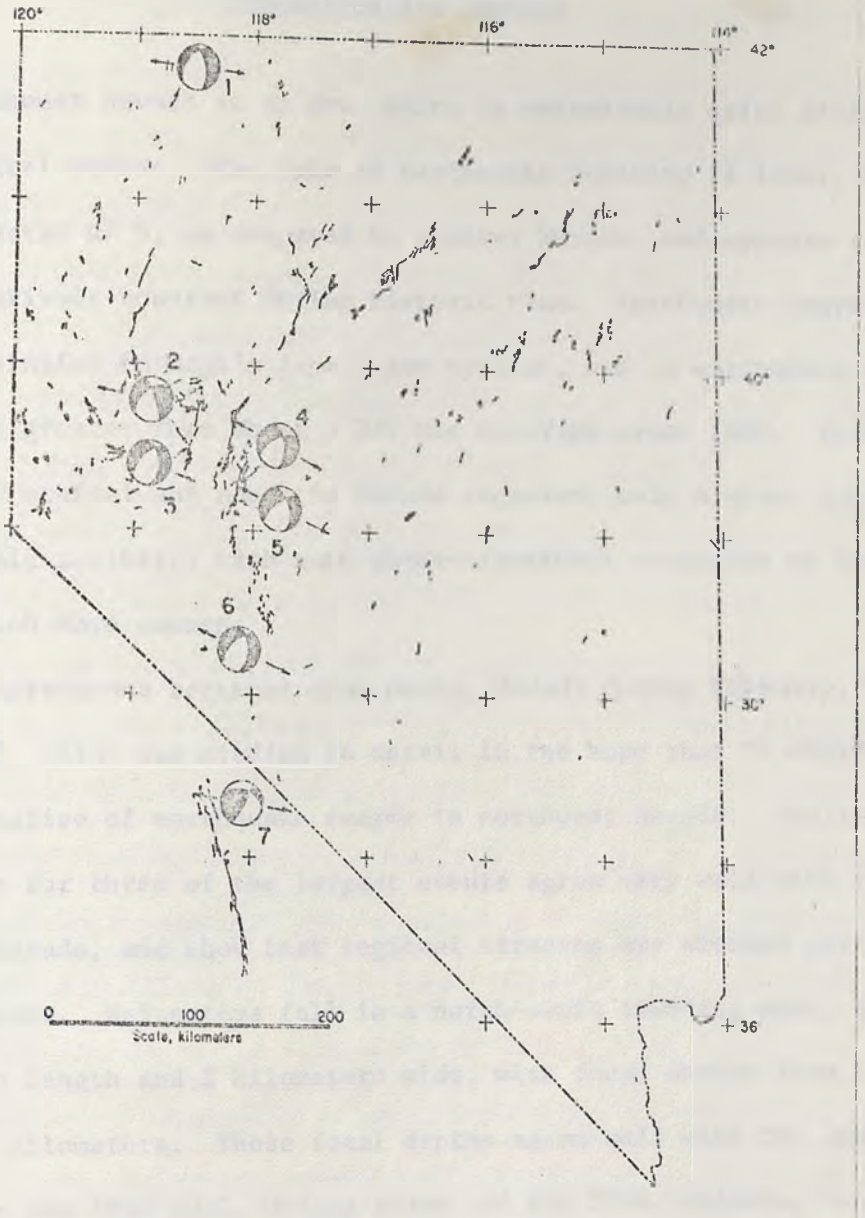

Figure 15. Earthquake mechanism plots for western Nevada showing each tension axis.

Chapter 3

DISCUSSION AND SUMMARY

Northwest Nevada is an area which is seismically quite different from central Nevada. The rate of earthquake activity is lower, by more than a factor of 5, as compared to central Nevada; and appears to have been relatively constant during historic time. Earthquake swarm sequences similar to Mogi's type 3 are typical, and no earthquake with magnitude greater than about 5 3/4 has occurred since 1860. Earthquake swarms in central and southern Nevada represent only a minor part of the seismic activity, with main shock-aftershock sequences or isolated events much more common.

An earthquake sequence near Denio, Nevada during February, March, and April, 1973, was studied in detail in the hope that it would be representative of earthquake swarms in northwest Nevada. Fault-plane solutions for three of the largest events agree very well with those of western Nevada, and show that regional stresses are similar over much of the state. Epicenters fall in a north-south trending zone, 8 kilometers in length and 2 kilometers wide, with focal depths from 5 1/2 to 8 1/2 kilometers. These focal depths agree well with the depths found for the 1968 Adel, Oregon swarm and the 1966 Caliente, Nevada sequence, as discussed by Ryall and Savage (1969). Aftershocks of the 1954 Fairview Peak earthquake generally have depths ranging from 12 to 14 kilometers (Stauder and Ryall, 1967). Earthquakes in northwest Nevada seem to be somewhat shallower than earthquakes in central Nevada. The b-value for this sequence is 1.09, which is considerably

higher than 0.81 for northwest Nevada as a whole.

The results of this investigation indicate that the 1973 Denio earthquake swarm as well as other swarms in northwest Nevada may be the result of, or at least correlate with, the local geothermal activity often present in this part of the state. In geothermal areas, water probably circulates to depths of several kilometers, and fluid flow can be expected to the depths of the earthquakes of the Denio swarm. Most of the events located in the geothermal areas of Iceland by Ward and Bjornsson (1971) had depths between 2 and 6 kilometers. Circulating water, especially at high temperatures causes stress corrosion. The high tensile stresses at the ends of the fractures enhance the corrosive action of the water and tend to lengthen them.

The relatively high b-value of 1.00 found for this earthquake swarm can possibly be explained as the result of several factors. Wyss (1973) found that b-values increased with increase in local pore pressure. High pore pressures can be expected to exist if geothermal waters are circulating at depth. Mogi (1966) showed that b-values increase with the degree of heterogeneity of the rock. This heterogeneity in the Denio area could be explained by the complicated volcanic geology and any fracturing that would accompany a recent intrusive body. Scholz (1968a) showed that high b-values are observed at low to moderate stress levels. If the rock in this area is weakened to the point where only moderate-sized stresses can occur, then this condition is also met.

A possible connection between earthquake swarms and geothermal activity in northwest Nevada exists. The rock could be weakened by

fracturing caused by any intrusive bodies, and by the effects of stress corrosion and leaching caused by geothermal fluids. The length of the fractures would be limited by fluctuations in the stress field, caused by inhomogeneities in the rock. The rock would then fracture in response to the regional stress and there would be small to moderate sized-earthquakes, as the rock would lack the strength necessary to sustain stresses that result in large main shock-aftershock sequences.

While the suggestion has been made that earthquake swarms in this part of Nevada are somehow linked to geothermal activity, other explanations for the occurrence of these swarms have by no means been ruled out. Detailed studies of swarm phenomena could lead to a better understanding of this relationship. The historic record, as well as the results of this study suggests that there may be an upper limit, of perhaps 5 3/4 to 6, to the magnitude of earthquakes in this part of Nevada. If a connection between geothermal activity and earthquake swarms, as well as the possible upper limit to earthquake magnitude can be confirmed by further studies, such knowledge would be extremely useful for engineering purposes, including nuclear reactor siting.

The University of Nevada Seismological Laboratory has recently installed four telemetering short-period seismographic stations in northwest Nevada, to improve our ability to detect and locate small earthquakes in the area. One of these stations is located 18 kilometers southwest of the center of activity of the 1973 Denio swarm. This station was recording local events, probably from the same area as the swarm, as late as April, 1974, at the rate of approximately 2 or 3 detectable events per week. Because these swarms appear to last at

least as long as a year, close monitoring of the seismic activity of areas of interest should locate recent swarms. Detailed microearthquake studies of these areas are suggested for further work.

APPENDIX I

The Geiger Least-Squares Method

The following is a detailed description of the method used in the LOC computer program to adjust the trial hypocenter. Holding the origin time fixed, the X, Y and Z coordinates are adjusted by the least-squares method to a point where they best fit the data.

Definitions:

X_o, Y_o, Z_o the cartesian grid coordinates of the hypocenter

t_o the origin time of the earthquake

X_i, Y_i, Z_i the station grid coordinates

t_i the computed P-wave arrival time at station i

T_i the computed traveltime of a P-wave to station i

F_i the arrival time anomaly at station i

The origin time, t_o, is calculated using the S-P time of each event and is not adjusted by the least squares routine. Thus t_i is a function only of the hypocenter coordinates X_o, Y_o, Z_o. Small changes in t_i due to small changes in X_o, Y_o, Z_o can be expressed by the following Taylor's expansion:

(1) $$dt_i = \frac{\partial t_i}{\partial X_o} dX_o + \frac{\partial t_i}{\partial Y_o} dY_o + \frac{\partial t_i}{\partial Z_o} dZ_o$$

F_i the arrival time anomaly at station i, can be written in the form:

(2) $$F_i = E_i + dt_i$$

In this equation, dt_i is the calculated change in arrival time due to an adjustment of dX_o, dY_o, dZ_o in the hypocenter and E_i is the arrival time anomaly after this adjustment.

From (1) and (2), we have:

(3) $$\frac{\partial t_i}{\partial X_0} dX_0 + \frac{\partial t_i}{\partial Y_0} dY_0 + \frac{\partial t_i}{\partial Z_0} dZ_0 - F_i = -E_i$$

By definition:

$t_i = T_i + t_0$ therefore

$$\frac{\partial t_i}{\partial X_0} = \frac{\partial T_i}{\partial X_0}, \quad \frac{\partial t_i}{\partial Y_0} = \frac{\partial T_i}{\partial Y_0}, \quad \frac{\partial t_i}{\partial Z_0} = \frac{\partial T_i}{\partial Z_0}$$

Substituting into (3), we get:

(4) $$\frac{\partial T_i}{\partial X_0} dX_0 + \frac{\partial T_i}{\partial Y_0} dY_0 + \frac{\partial T_i}{\partial Z_0} dZ_0 - F_i = -E_i$$

Let:

$$\alpha_i = \frac{\partial T_i}{\partial X_0}, \quad \beta_i = \frac{\partial T_i}{\partial Y_0}, \quad \gamma_i = \frac{\partial T_i}{\partial Z_0}$$

$$Y_1 = dX_0, \quad Y_2 = dY_0, \quad Y_3 = dZ_0$$

Then (4) becomes:

(5) $$\alpha_i Y_1 + \beta_i Y_2 + \gamma_i Y_3 - F_i = -E_i$$

We want to calculate Y_1, Y_2, Y_3 such that the sum of the squares of the residuals of observed vers computed arrival times is a minimum. That is:

$$\sum E_i^2 = \text{a minimum}$$

To minimize this we want:

(6) $$\frac{\partial}{\partial Y_j}\left[\sum_{i=1}^{N} E_i^2\right] = 0$$ where j = 1, 3 and

N = the number of stations

Note that equation (6) can be written as:

(7) $$\sum_{i=1}^{N} E_i \frac{\partial E_i}{\partial Y_j} = 0$$ where j = 1, 3

From equation (5):

$$(8)\qquad \frac{\partial E_i}{\partial Y_1} = -\alpha_i, \qquad \frac{\partial E_i}{\partial Y_2} = -\beta_i, \qquad \frac{\partial E_i}{\partial Y_3} = -\gamma_i$$

Using equations (7) and (8), we get:

$$(9)\qquad \begin{aligned} &\alpha_1 E_1 + \alpha_2 E_2 + \alpha_3 E_3 + \cdots + \alpha_N E_N = 0, \quad \text{for } j = 1 \\ &\beta_1 E_1 + \beta_2 E_2 + \beta_3 E_3 + \cdots + \beta_N E_N = 0, \quad \text{for } j = 2 \\ &\gamma_1 E_1 + \gamma_2 E_2 + \gamma_3 E_3 + \cdots + \gamma_N E_N = 0, \quad \text{for } j = 3 \end{aligned}$$

Now using equation (9) for j = 1 and equation (5) and expanding, we get:

$$(10)\qquad \begin{aligned} &\alpha_1\alpha_1 Y_1 + \alpha_1\beta_1 Y_2 + \alpha_1\gamma_1 Y_3 - \alpha_1 F_1 \\ &+ \alpha_2\alpha_2 Y_1 + \alpha_2\beta_2 Y_2 + \alpha_2\gamma_2 Y_3 - \alpha_2 F_2 \\ &+ \\ &\vdots \\ &+ \alpha_N\alpha_N Y_1 + \alpha_N\beta_N Y_2 + \alpha_N\gamma_N Y_3 - \alpha_N F_N \\ &= 0 \end{aligned}$$

Similar equations for j = 2 and 3 can be written. These equations can be written in the following form, noting that each term is summed over i individually:

$$(11)\quad [\alpha_i\ \alpha_i]\,Y_1 + [\alpha_i\ \beta_i]\,Y_2 + [\alpha_i\ \gamma_i]\,Y_3 - [\alpha_i\ F_i] = 0;\ j=1$$

$$[\beta_i\ \alpha_i]\,Y_1 + [\beta_i\ \beta_i]\,Y_2 + [\beta_i\ \gamma_i]\,Y_3 - [\beta_i\ F_i] = 0;\ j=2$$

$$[\gamma_i\ \alpha_i]\,Y_1 + [\gamma_i\ \beta_i]\,Y_2 + [\gamma_i\ \gamma_i]\,Y_3 - [\gamma_i\ F_i] = 0;\ j=3$$

Let:

$$A_{11} = \Sigma\,\alpha_i\alpha_i\ ,\quad A_{12} = \Sigma\,\alpha_i\beta_i\ ,\quad A_{13} = \Sigma\,\alpha_i\gamma_i$$

$$A_{21} = \Sigma\,\beta_i\alpha_i\ ,\quad A_{22} = \Sigma\,\beta_i\beta_i\ ,\quad A_{23} = \Sigma\,\beta_i\gamma_i$$

$$A_{31} = \Sigma\,\gamma_i\alpha_i\ ,\quad A_{32} = \Sigma\,\gamma_i\beta_i\ ,\quad A_{33} = \Sigma\,\gamma_i\gamma_i$$

and

$$B_1 = \Sigma\,\alpha_i F_i\ ,\quad B_2 = \Sigma\,\beta_i F_i\ ,\quad B_3 = \Sigma\,\gamma_i F_i$$

Now equations (11) can be written in matrix form:

$$\begin{bmatrix} A_{11} & A_{12} & A_{13} \\ A_{21} & A_{22} & A_{23} \\ A_{31} & A_{32} & A_{33} \end{bmatrix} \cdot \begin{bmatrix} Y_1 \\ Y_2 \\ Y_3 \end{bmatrix} = \begin{bmatrix} B_1 \\ B_2 \\ B_3 \end{bmatrix}$$

These equations are now solved for the hypocenter adjustments Y_1, Y_2, Y_3 using Cramer's rule. If no solution can be found, the program fixes the depth Z, at the preceding value and attempts to solve for Y_1, Y_2, having set $Y_3 = 0$. If no solution can be found for either case, the program prints out "DEGENERATE" and begins processing the next event.

APPENDIX II

Calculating Traveltime and the Derivatives of the Traveltime

The CAL subroutine in the LOC program computes the traveltimes and derivatives of the traveltimes with respect to the given hypocentral coordinates for each station. The earth model used is one of horizontal constant velocity layers. It is assumed that the earthquake is close enough to all stations so that the first P-wave arrival is a direct wave refracted at the boundaries between velocity layers.

The subroutine first finds which layer the trial hypocenter is in and then calculates the angle of incidence of the ray at the focus, Θ_j as a function of travel time and epicentral distance to station I. CAL then calculates the travel time, T (I), for an epicentral distance DEL (I) corresponding to station I. Finally, the partial derivatives of T (I) with respect to X_o, Y_o and Z_o are found. The subroutine then returns these values to the main program.

Definitions:

DEL (I)	the epicentral distance to station I
Layer J	the layer containing the hypocenter
TKJ	the depth trial hypocenter is into layer J
XBIG	the upper limit for a point where the direct wave from the focus leaves layer J
XLIT	the lower limit for the same point
Θ_j	the angle of incidence from focus

A diagram of the following can be seen in figure 16.

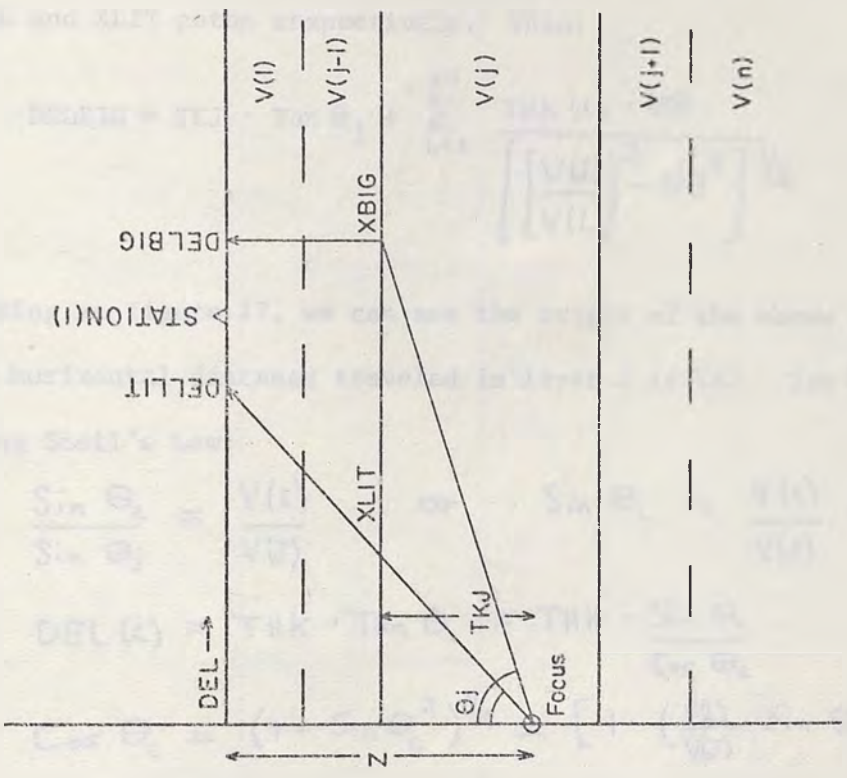

Figure 16. Diagram explaining the CAL subroutine.

Let:

XBIG = DEL (I), assuming vertical refraction at the boundaries

XLIT = DEL (I) · TKJ/Z, assuming no refraction

Note that $\mathrm{Sin}\,\Theta_j$ for the XBIG and XLIT paths are UB and UL respectively and:

$$UB = XBIG/(XBIG^2 + TKJ^2)^{1/2}$$

$$UL = XLIT/(XLIT^2 + TKJ^2)^{1/2}$$

Let DELBIG and DELLIT be the values of DEL corresponding to the XBIG and XLIT paths respectively. Then:

$$DELBIG = TKJ \cdot \mathrm{Tan}\,\Theta_j + \sum_{L=1}^{j-1} \frac{THK(L) \cdot UB}{\left[\left[\frac{V(J)}{V(L)}\right]^2 - UB^2\right]^{1/2}}$$

Looking at figure 17, we can see the origin of the above equation. The horizontal distance traveled in layer J is $TKJ \cdot \mathrm{Tan}\,\Theta_j$.

Using Snell's Law:

$$\frac{\mathrm{Sin}\,\Theta_L}{\mathrm{Sin}\,\Theta_j} = \frac{V(L)}{V(J)} \qquad \text{or} \qquad \mathrm{Sin}\,\Theta_L = \frac{V(L)}{V(J)}\,\mathrm{Sin}\,\Theta_j$$

$$DEL(L) = THK \cdot \mathrm{Tan}\,\Theta_L = THK \cdot \frac{\mathrm{Sin}\,\Theta_L}{\mathrm{Cos}\,\Theta_L}$$

$$\mathrm{Cos}\,\Theta_L = (1 - \mathrm{Sin}\,\Theta_L^2)^{1/2} = \left[1 - \left(\frac{V(L)}{V(J)}\,\mathrm{Sin}\,\Theta_j\right)^2\right]^{1/2}$$

$$DEL(L) = \frac{THK \cdot \frac{V(L)}{V(J)}\,\mathrm{Sin}\,\Theta_j}{\left[1 - \left(\frac{V(L)}{V(J)}\,\mathrm{Sin}\,\Theta_j\right)^2\right]^{1/2}}$$

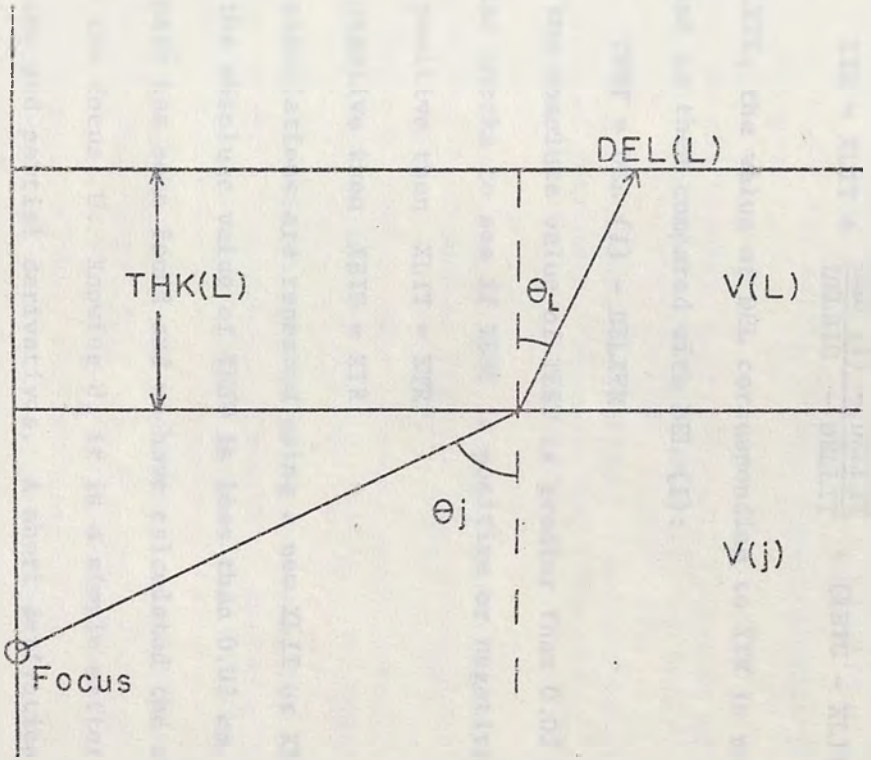

Figure 17. Diagram explaining the CAL subroutine.

or:

$$DEL\ (L) = \frac{THK\ (L) \cdot UB}{\left[\left(\frac{V(J)}{V(L)}\right)^2 - UB^2\right]^{1/2}}$$

A value for DEL (L) is found for each layer and added to get the total horizontal distance traveled by a ray through XBIG. Similarly, DELLIT is calculated for XLIT.

A point between XLIT and XBIG is now chosen:

$$XTR = XLIT + \frac{DEL\ (I) - DELLIT}{DELBIG - DELLIT} \cdot (XBIG - XLIT)$$

DELXTR, the value of DEL corresponding to XTR is now calculated. This value is then compared with DEL (I):

TEST = DEL (I) - DELXTR

If the absolute value of TEST is greater than 0.02 km, then the subroutine checks to see if TEST is positive or negative:

If positive then XLIT = XTR

If negative then XBIG = XTR

Now the calculations are repeated using a new XLIT or XBIG.

If the absolute value of TEST is less than 0.02 km, then the correct path has been found and we have calculated the angle of incidence at the focus, U. Knowing U, it is a simple matter to find the travel time and partial derivatives. A short derivation of the method used to calculate these can be found in the description of the HYPOLAYR program by J. P. Eaton (Eaton, 1969).

BIBLIOGRAPHY

Douglas, B. M. and A. Ryall (1972). Spectral characteristics and stress drop for microearthquakes near Fairview Peak, Nevada, J. Geophys. Res., 77(2), 351-359.

Eaton, Jerry P. (1963). Crustal structure from San Francisco, California, to Eureka, Nevada, from seismic-refraction measurements, J. Geophys. Res., 68(20), 5789-5806.

Eaton, Jerry P. (1969). HYPOLAYR, a computer program for determining hypocenters of local earthquakes in an earth consisting of uniform flat layers over a half space, Open File Report, U. S. Geological Survey, 155 p.

Eaton, J. P. and K. J. Murato (1960). How volcanoes grow, Science, 132, 925-938.

Gutenberg, B. and Richter, C. F. (1944). Frequency of earthquakes in California, Bull. Seism. Soc. Am., 34, 185-188.

Gutenberg, B. and Richter, C. F. (1954). Seismicity of the earth and associated phenomena, Princeton University Press, Princeton, New Jersey.

Healy, J. H., W. W. Rudey, D. T. Griggs, and C. B. Raleigh (1968). The Denver earthquakes, Science, 161, 1301-1310.

Horton, Robert C. (1964). Hot springs, sinter deposits, and volcanic cinder cones in Nevada. Map 25, Nev. Bur. of Mines.

Koizumi, C. J., A. Ryall, and K. F. Priestley (1973). Evidence for a high-velocity lithospheric plate under northern Nevada, Bull. Seism. Soc. Am., 63(b), 2135-2144.

Langenheim, R. L. and E. R. Larson (1973). Correlation of great basin stratigraphic units, Bull. 72, Nev. Bur. of Mines.

Meister, Laurent J. (1966). Seismic refraction study of Dixie Valley, Nevada, Part I of final scientific report AFCEL-66-848 prepared for Air Force Cambridge Research Laboratories, pp. i-viii, 1-72.

Mogi, K. (1962). On the time distribution of aftershocks accompanying the recent major earthquakes in and near Japan, Bull. Earthquake Res. Inst. Tokyo Univ., 40, 107-124.

Mogi, K. (1966). Earthquakes and fractures, Tectonophysics, 5, 35-55.

Norris, R. A., and R. H. Johnson (1969). Submarine volcanic eruptions recently located in the Pacific by Sofar hydrophones, J. Geophys. Res., 74, 650-664.

Ryall, A., D. B. Slemmons, and L. D. Gedney (1966). Seismicity, tectonism and surface faulting in the western United States during historic time, Bull. Seism. Soc. Am., 56(5), 1105-1135.

Ryall, A., A. E. Jones, and J. D. Van Wormer (1968). Triggering of microearthquakes by earth tides and other features of the Truckee, California, earthquake sequence of September, 1966, Bull. Seism. Soc. Am., 58, 215-248.

Ryall, A. and W. U. Savage (1969). A comparison of seismological effects for the Nevada underground test BOXCAR and natural earthquakes in the Nevada region, J. Geophys. Res., 74(17), 4281-4289.

Ryall, A. and S. D. Malone (1971). Earthquake distribution and mechanism of faulting in the Rainbow Mountain - Dixie Valley - Fairview Peak area, central Nevada, J. Geophys. Res., 76(29), 7241-7248.

Ryall, A. and B. M. Doublas (1974). Seismicity of northwest Nevada related to the feasibility of power plant siting. Report to Sierra Pacific Power Company, Reno, Nevada.

Sass, J. H., A. H. Lachenbruck, R. J. Munroe, G. W. Greene, and T. H. Moses, Jr. (1971). Heat flow in the western United States, J. Geophys. Res., 76(26), 6376-6413.

Savage, William U. (1972). Microearthquake clustering near Fairview Peak, Nevada, and in the Nevada Seismic Zone, J. Geophys. Res., 77(35), 7049-7056.

Savage, William U. (1974). Unpublished PhD Thesis, Univ. of Nevada.

Sbar, M. L., M. Barazangi, J. Dorman, C. H. Scholz, R. B. Smith (1972). Tectonics of the intermountain seismic belt, western United States: microearthquake seismicity and composite fault plane solutions, Geol. Soc. Amer. Bull., 83, 13-28.

Scholz, C. H. (1968a). The frequency-magnitude relation of microfracturing in rock and its relation to earthquakes, Bull. Seism. Soc. Am., 58, 399-415.

Scholz, C. H. (1968b). Mechanism of creep in brittle rock, J. Geophys. Res., 73(10), 3295-3302.

Slemmons, D. B., A. E. Jones, and J. I. Gimlet (1965). Catalog of Nevada earthquakes, 1852-1960, Bull. Seism. Soc. Am., 55(2), 537-583.

Stauder, William S. J., and A. Ryall (1967). Spatial distribution and source mechanism of microearthquakes in central Nevada, Bull. Seism. Soc. Am., 57(6), 1317-1345.

Sykes, Lynn R. (1970). Earthquake swarms and sea-floor spreading, J. Geophys. Res., 75(32), 6598-6611.

Utsu, Tokuji (1971). Aftershocks and earthquake statistics (III), J. Fac. Sci., Hokkaido Univ., Ser. VII (Geophysics), 3(5),

Ward, P. L. and S. Bjornsson (1971). Microearthquakes, swarms and the geothermal areas of Iceland, J. Geophys. Res., 76(17), 3953-3982.

Wyss, Max (1973). Towards a physical understanding of the earthquake frequency distribution, Geophys. J. R. Astr. Soc., 31, 341-359.